European Journal of Radiology 114 (2019) 1–5

Contents lists available at ScienceDirect

European Journal of Radiology

journal homepage: www.elsevier.com/locate/ejrad

Improved visualization of the coronary arteries using motion correction during vasodilator stress CT myocardial perfusion imaging

Bhavna Balaney[a], Mani Vembar[b], Michael Grass[c], Amita Singh[a], Keigo Kawaji[a], Luis Landeras[a], Jonathan Chung[a], Victor Mor-Avi[a], Amit R. Patel[a,*]

[a] Departments of Medicine and Radiology, University of Chicago Medical Center, Chicago, IL, United States
[b] Department of CT Clinical Science, Philips Healthcare, Cleveland, OH, United States
[c] Philips Research, Hamburg, Germany

ARTICLE INFO

Keywords:
Coronary computed tomography
Noninvasive coronary angiography
Myocardial perfusion imaging
Vasodilator stress testing

ABSTRACT

Background: Vasodilator stress computed tomography perfusion (sCTP) imaging is complementary to coronary CT angiography (CCTA), used to determine the hemodynamic significance of coronary artery disease. However, it requires a separate image acquisition due to motion artifacts caused by higher heart rates during stress, resulting in increased iodine contrast dose and radiation. We sought to determine whether a novel motion correction algorithm applied to stress images would improve the visualization of the coronary arteries to potentially allow CCTA + sCTP evaluation in a single scan.

Methods: 28 patients referred for clinically indicated CCTA (iCT, Philips) underwent sCTP imaging (retrospective-gating with dose modulation; 100 kVp and 250 mA; 5.2 ± 4.3 mSv) after regadenoson (0.4 mg, Astellas). Stress images were reconstructed using standard filtered back-projection (FBP) and also processed to generate interaction-free coronary motion-compensated back-projection reconstructions (MCR). Each coronary artery from standard FBP and MCR images was viewed side-by-side by a reader blinded to the reconstruction technique, who graded severity of motion artifact by segment (scale 0–5, with 3 as the threshold for diagnostic quality) and to measure signal-to-noise and contrast-to-noise ratios (SNR, CNR).

Results: Visualization scores were higher with MCR for all coronary segments, including 14/86 (16%) segments deemed as non-diagnostic on FBP images. SNR (7 ± 2) and CNR (15 ± 8) were unchanged by motion-correction (7 ± 3, p = 0.88 and 15 ± 5, p = 0.94, respectively).

Conclusions: MCR improves the visualization of coronary anatomy on sCTP images without degrading image characteristics. This algorithm is an important step towards the combined assessment of coronary anatomy and myocardial perfusion in a single scan, which will reduce study time, radiation exposure and contrast dose.

1. Introduction

Cardiac computed tomography (CT) is a versatile imaging modality that can be used to evaluate coronary artery stenosis, left ventricular (LV) size and function, and myocardial perfusion. Nevertheless, cardiac CT imaging is predominantly used as an alternative to invasive coronary angiography, which can accurately assess the presence and severity of coronary artery stenosis [1,2], while the hemodynamic significance of the detected stenosis is usually determined separately using other techniques, such as myocardial perfusion imaging or invasive angiography with fractional flow-reserve measurements.

Although computed tomography perfusion (CTP) imaging has been shown to be a useful diagnostic tool [3–5], this technique requires an additional scan at peak vasodilator stress, which results in increased radiation and iodine contrast dose, compared to the typical protocol of computed tomography angiography (CTA) of the coronary arteries alone. This is because imaging only once during stress, rather than using two consecutive scans, would hinder the assessment of coronary anatomy due to increased motion artifacts with higher heart rates induced by vasodilators. In clinical practice, coronary motion during resting imaging is mitigated by the use of beta-blockers. However, at peak vasodilator stress, this is not possible.

Despite considerable efforts to prevent motion artifacts by increasing the temporal resolution of the scanners and refining reconstruction algorithms, this remains a major limitation of CTA, especially in coronary segments that are subject to considerable motion

* Corresponding author at: University of Chicago Medical Center, 5758 South Maryland Ave., MC 9067, Chicago, IL, 60637, United States.
E-mail address: amitpatel@uchicago.edu (A.R. Patel).

https://doi.org/10.1016/j.ejrad.2019.02.010
Received 27 November 2018; Received in revised form 12 January 2019; Accepted 11 February 2019

even during relatively quiescent phases of the cardiac cycle, such as diastasis, when CTA images are usually acquired. Further technological improvements are needed to effectively solve this problem [6–12]. If found, such a solution could theoretically allow comprehensive evaluation of both the presence and severity of coronary stenosis, as reflected by the degree of luminal narrowing and the extent of the resultant perfusion defect, from images obtained in a single scan during peak stress. In this study, we sought to test a novel motion correction algorithm designed to improve the quality of stress CTP images, as a step towards achieving this goal.

2. Methods

2.1. Population and study design

We prospectively enrolled 34 patients with symptoms suggesting of coronary artery disease referred to undergo CTP imaging during vasodilator stress (regadenoson 0.4 mg IV bolus; Astellas, Northbrook, IL). We excluded patients with prior coronary artery bypass grafting, pacemaker and contraindications to coronary CTA, including known allergies to iodine, renal dysfunction (creatinine > 1.6 mg/dL), inability to perform a 10-second breath-hold, and contraindications to beta-blockers or regadenoson, such as chronic obstructive pulmonary disease, advanced heart block, or systolic blood pressure < 90 mm Hg. The study was approved by the Institutional Review Board, and each patient provided written, informed consent before participation.

The quality of visualization of the coronary arteries was compared between images reconstructed using conventional methodology against those reconstructed using the novel motion-compensated reconstruction (MCR). In addition, signal to noise ratio (SNR) and contrast to noise ratio (CNR) were measured for both types of images to assess the effects of motion correction on these images and evaluate for image degradation.

2.2. Image acquisition and reconstruction

After standard resting clinical CT angiography imaging was completed, CTP imaging was performed with a 256-slice multidetector CT scanner (Brilliance iCT, Philips Healthcare, Cleveland OH, USA) with a detector configuration of 128 x 0.625 mm and 0.27 s rotation time. Images were acquired 1 min after the administration of regadenoson (Astellas) (0.4 mg, intravenously) which was used to induce hyperemia. Stress scans were performed using a retrospectively-gated helical protocol. A tube voltage of 100 kVp and an effective tube current-time product of 250 mAs was used. To reduce radiation dose, ECG tube current modulation was used with maximum tube output at the end-systolic phase (corresponding to 40% of the cardiac cycle), because at higher heart rates coronary motion is expected to be lowest during this part of the cardiac cycle. Contrast enhancement was achieved by a 50–70 mL bolus of iodinated contrast (adjusted for body weight) at a rate of 4 mL/s. Image acquisition was triggered by the appearance of contrast in the descending thoracic aorta (5 s after attenuation increase > 50 Hounsfield units [HU] over baseline was detected). The resulting effective radiation dose for stress imaging was 5.2 ± 4.3 mSv, including both the resting CT angiography and stress perfusion imaging.

Images obtained during stress were reconstructed targeting the end-systolic phase. After standard FBP reconstructions were generated, the raw projection data were processed off-line to generate coronary MCR datasets [13]. First, an image volume (i.e., a region of interest) comprising of cardiac phases ± 5%, ± 10% on either side of the targeted physiologic phase was generated [14], to which vessel enhancement filtering was applied to enhance dense tubular structures, such as coronary vessels [15]. Following this, an elastic registration was performed between the targeted and all neighboring phases within the cardiac volume, resulting in a motion vector field on a per voxel basis that describes voxel displacement from the target to all neighboring phases. Finally, motion-corrected images were generated by applying the motion vector field during the back-projection process [16]. Motion was corrected during the weighting steps and in the back-projection process itself. Additional technical details are described elsewhere [17,18]. Slices were reconstructed with a thickness of 0.8 mm at an increment of 0.4 mm for both FBP and MCR datasets.

2.3. Image analysis

Image analysis was performed by a board-certified cardiologist with level III certification in cardiac CT. FBP and MCR images were viewed side-by-side and windowed simultaneously, and the thinnest reconstruction without maximum intensity projection was evaluated. The reader, who was blinded to the reconstruction technique, graded the severity of motion artifact for every one of 10 coronary artery segments. These included: left main (LM), proximal left anterior descending (LAD) (up to the takeoff of the first diagonal branch), mid LAD (from first diagonal to second diagonal branch), distal LAD (beyond takeoff of the second diagonal branch), proximal left circumflex (LCx), distal LCx, the major obtuse marginal branch or ramus intermedius (OM), proximal right coronary artery (RCA), mid RCA, and distal RCA.

Each segment was graded on a scale from 0 to 5 to describe severity of motion artifact and suitability for interpretation as follows: 0 - vessel too small to measure (< 2 mm); 1 - barely visible; 2 - visible with poor image quality; 3 - visible with fair image quality; 4 - visible with good image quality; 5 - visible with excellent image quality. Threshold of 3 was noted to be adequate for diagnosis and interpretation. The score of each of the 10 evaluated coronary segments was summed to derive a total image quality score for each patient for both the FBP and MCR images.

To calculate the SNR and CNR, mean values and standard deviations of x-ray attenuation in Hounsfeld units (HU) were measured in two regions of interest drawn in the proximal RCA and the epicardial fat next to the proximal RCA. CNR was calculated as a ratio between the mean HU in the proximal RCA and the epicardial fat [19]. In addition, a region of interest with an area of 100mm^2 was drawn in the ascending aorta near the takeoff of the LM coronary artery to assess degree of contrast opacification. SNR was calculated as a ratio between the mean HU value (representing the signal intensity) and the standard deviation (reflecting the noise level).

2.4. Statistical analysis

Continuous variables are presented as mean ± SD, and categorical variables as numbers and percentages. Visualization quality scores for each of the 10 coronary segments were compared between the FBP and MCR images, as well as the overall score for each patient, using paired t-tests, after having ascertained the normal distribution of the data. Linear regression was used to evaluate the relationships between contrast opacification of the aorta, SNR, CNR, and the visualization scores.

3. Results

After excluding 6 patients with poor contrast opacification, a total of 28 patients who were ultimately included in the analysis. Their baseline characteristics were: age 54 ± 9; 56% males; BSA 2.0 ± 0.5 m^2; 21 with hypertension, 13 with dyslipidemia, 7 with diabetes mellitus, 3 with known coronary artery disease, 10 with smoking history. The mean heart rate during peak vasodilator stress was 86 ± 11 bpm (range 68–114 bpm) and the systolic blood pressure was 112 ± 15 mmHg (range 84–139 mmHg).

Fig. 1 shows examples of perfusion images reconstructed using the standard FBP technique, which were obtained in 5 different study patients that received coronary visualization scores from 1 to 5. Of all 28 patients' coronary artery segments, there were 86/280 segments (31%)

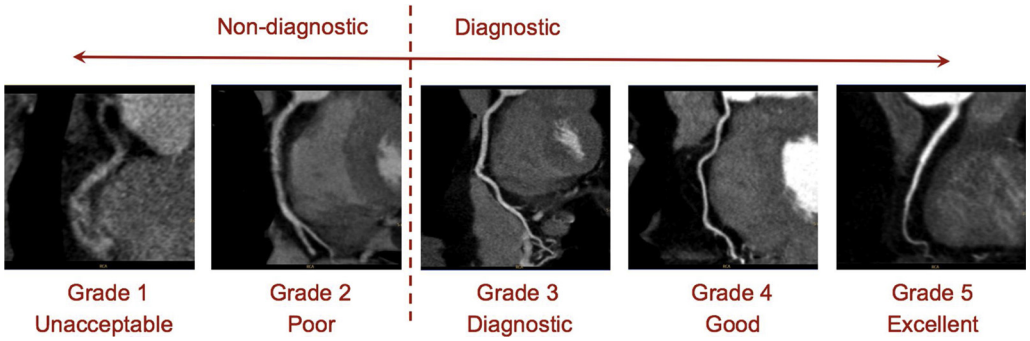

Fig. 1. Examples of stress perfusion images reconstructed using standard FBP technique obtained in 5 different study patients that received coronary visualization scores from 1 to 5.

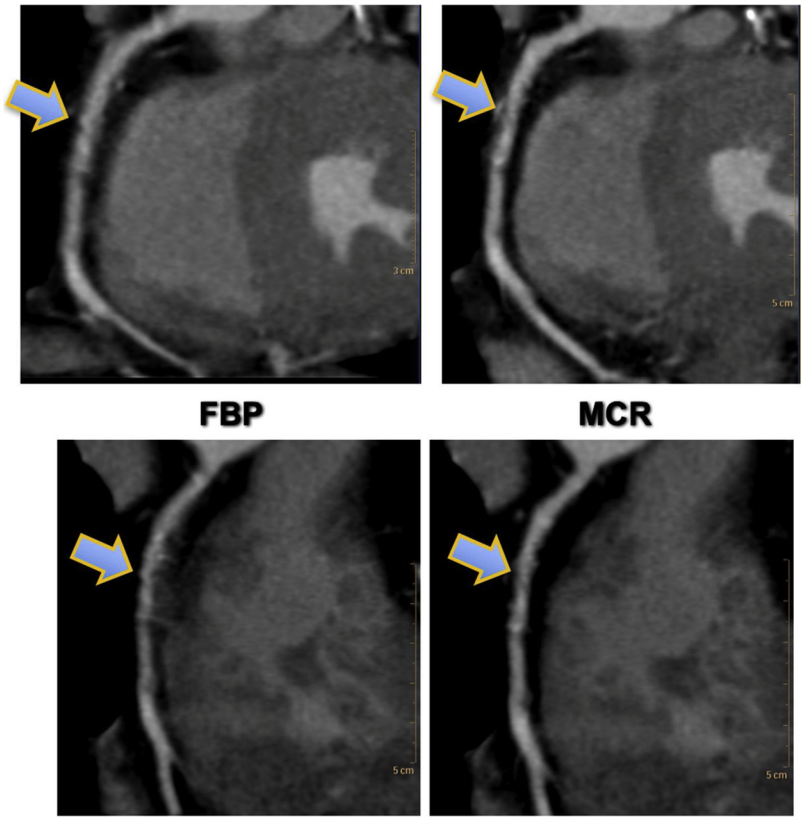

Fig. 2. Example of stress perfusion images reconstructed using standard FBP technique (left) and the corresponding MCR images (right) obtained in two study patients, depicting the improvement in the visualization of the right coronary artery with motion correction (see text for details).

that were graded as non-diagnostic (score of < 3). The summed visualization score for all 10 coronary artery segments was 28.1 ± 6.7 (range 16 to 43; median value 27.5), out of a maximum possible 50 in each patient.

Fig. 2 shows examples of perfusion images reconstructed using the standard FBP technique and the corresponding MCR images obtained in two patients. While the proximal and mid segments of the RCA look blurred on the FBP images, the arteries appear better defined with sharper boundaries after motion correction. With MCR, the total summed visualization score improved to 30.3 ± 6.9 (range 18–44; median value 30.5); this improvement was highly statistically significant (= 0.00003). Importantly, of the 86 segments with non-diagnostic image quality (score < 3) on FBP images, 14 segments (16%) improved by at least one grade by using the MCR approach. Also important is the fact that no segments deemed as diagnostic on FBP images (score 3 or above) became non-diagnostic with MCR.

Coronary artery segmental visualization scores and the number of patients with non-diagnostic segments for both the FBP and MCR images are shown in Table 1. With the FBP reconstruction, of the 10 segments, the LM was non-diagnostic in the smallest number of patients (2/28 or 7%), and the mean visualization score was the highest. In contrast, the largest number of non-diagnostic images was noted for the distal LAD and OM coronary segments (16/28 or 57%), and these two segments received the lowest visualization scores. Importantly, with MCR, the number of non-diagnostic images was reduced in the majority of segments (6/10). The mean segmental visualization scores increased in all 10 segments, with the difference being statistically significant in 7 out of 10, approaching significance in 2 out of 10 (proximal LAD and OM) and not being significant in one segment (LM), which was already well visualized with the standard FBP reconstruction in 26/28 patients (93%). MCR did not help in the remaining 2/28 cases.

The average SNR was 7 ± 2 in the FBP images and 7 ± 3 in the MCR images (p = 0.88). Similarly, CNR did not change significantly from FBP to MCR in CNR: 15 ± 8 versus 15 ± 5 (p = 0.94). Average

Table 1
Coronary artery segmental visualization scores and the number of patients with non-diagnostic segments for the standard filtered back-projection (FBP) and motion corrected reconstruction (MCR) images.

Coronary Segment	Number of Patients with Non-Diagnostic Segments		Visualization Score by Segment		p-value (paired *t*-test)
	Standard FBP	Motion Corrected	Standard FBP	Motion Corrected	
LM	2	2	3.6 ± 0.7	3.7 ± 0.7	0.33
pLAD	3	3	3.4 ± 0.7	3.5 ± 0.7	0.08
mLAD	6	6	3.1 ± 0.9	3.3 ± 0.9	0.02
dLAD	16	14	1.8 ± 1.5	2.0 ± 1.7	0.01
pLCx	9	7	2.9 ± 1.0	3.1 ± 0.9	0.01
dLCx	14	12	2.3 ± 1.3	2.5 ± 1.4	0.02
OM	16	14	2.1 ± 1.5	2.3 ± 1.6	0.06
pRCA	5	3	3.1 ± 0.8	3.5 ± 0.7	< 0.01
mRCA	9	5	2.7 ± 1.0	3.1 ± 1.0	< 0.01
dRCA	6	6	3.0 ± 1.0	3.2 ± 1.1	0.03

Abbreviations: LM – left main, LAD – left anterior descending, LCx – left circumflex, RCA – right coronary artery; prefixes: pproximal, m – mid, d – distal.

x-ray attenuation in the aortic root was 318 ± 96 HU (range 124 to 509). There was no notable correlation between the degree of contrast opacification and improvement in coronary visualization score (r = -0.10). Similarly, there was no significant correlation between SNR (r = -0.10) or CNR (r = 0.17) and the contrast opacification. Finally, the change in either SNR or CNR from FBP to MCR images did not correlate with contrast opacification.

4. Discussion

This study was designed to test the ability of the new MCR algorithm that compensates for cardiac motion to improve the visualization of the coronary arteries by alleviating motion artifacts on end-systolic images acquired during vasodilator stress. This was motivated by the idea that these images could potentially be used to assess both coronary anatomy for detection of coronary stenosis severity simultaneously with myocardial perfusion for detection of stress-induced ischemia, all in a single test. We found that the MCR algorithm significantly improved coronary visualization scores assigned by a reader blinded to the reconstruction technique used. This improvement was noted in many segments that were suboptimally visualized on FBP images.

One might claim that the level of improvement in coronary visualization we found is only modest, as reflected by the small 2-unit increase in total summed score that spans a scale of 50 units. However, it is important to remember that segments that were sufficiently well visualized to allow confident diagnosis are not the target of this technological development, aimed specifically at reducing motion artifacts. Thus, one should mostly focus on the improvement in the visualization of the segments that are deemed non-diagnostic because of motion artifacts on FBP images. Importantly, in our study, improvement was noted in 16% of these segments. This included coronary artery segments that were deemed to be too small to assess. Thus, while additional refinements of this reconstruction technique would be needed, even using this first version of the MCR algorithm would allow one in six patients to potentially avoid further testing.

Of note, our study was not designed to answer the question whether this level of improvement is sufficient to allow the use of MCR images obtained during peak vasodilator stress instead of resting images, and whether their quality is good enough to provide a similar level of diagnostic confidence. As stated above, it is likely that further refinements of the reconstruction technique would be needed to achieve this goal. While the outcome of such technological developments remains to be determined in future studies that would involve testing of improved version of the MCR algorithm in larger groups of patients, this pilot study provides a signal that this approach is indeed effective in reducing motion artifacts and is thus a promising step towards the ultimate goal of simultaneous evaluation of coronary anatomy and its downstream hemodynamic effects in a single imaging test.

One noteworthy detail of our study design is that the MCR algorithm was tested on end-systolic images, rather than on images reflecting the diastolic rest period (diastasis), as is routinely done to minimize the same motion artifacts that the MCR algorithm aims to handle. This detail stemmed from the fact that our ultimate goal is to minimize motion artifacts on images acquired during peak vasodilator stress, when heart rates are elevated (typically 80 bpm or higher), and, as a result, the duration of the diastasis is too short to obtain motion free images, thus effectively eliminating the theoretical advantage of this phase of the cardiac cycle in terms of reduced motion [20]. In contrast, the composite end-systolic motion-free period including the duration of the isovolumetric relaxation time, although subject to a minor linear shortening, is relatively constant at these heart rates and thus may be more suitable for imaging [21–23].

It is not unlikely that data manipulations such as those involved in the MCR algorithm could theoretically alter the basic characteristics of the image and thus result in image degradation despite effective correction of motion artifacts. To rule out this possibility, we measured SNR and CNR in both FBP and MCR images, and also studied the relationships between these characteristics and the coronary visualization scores. We found that the differences in reconstruction algorithms did not result in significant differences in the above image characteristics, and that they were not related to visualization scores, supporting the notion that the MCR algorithm does not cause image degradation. Additional evidence to this effect is the finding that no coronary segments that were well visualized with FBP reconstruction became non-diagnostic with MCR processing.

5. Limitations

One limitation of this study is the relatively small sample, which was a result of the pilot nature of the study and the need to transfer very large amounts of raw CT data to the manufacturer, since the current version of the algorithm is not available at this time to users other than the developers. Another limitation is that under hyperemic conditions, contrast levels in the aortic root are typically lower than those seen in resting scans, and low enhancement could potentially impact the performance of the MCR algorithm, especially of the vessel enhancement filter. Finally, one might view the fact that image quality was graded by a single reader as a limitation. However, this was done for the sake of simplicity by avoiding the need to assess the level of inter-reader agreement, which was not the focus of this study. Importantly, to minimize the impact of the subjective nature of the assessment of image quality on the study, the reader was blinded to the reconstruction technique.

6. Conclusions

In summary, this pilot study tested the ability of a novel reconstruction algorithm that compensates for cardiac motion to improve the visualization of the coronary arteries by alleviating motion artifacts on end-systolic images acquired during vasodilator stress. We found that this novel approach can minimize motion artifacts resulting in improved visualization of the coronary arteries on images acquired during peak vasodilator stress by effectively salvaging some of the segments deemed non-diagnostic on FBP images. Further algorithmic improvements are needed to increase the success rates of this improvement. Additional studies are needed to determine whether this methodology could potentially lead to the development of a single CT-based test for combined evaluation of coronary stenosis and its hemodynamic significance.

Conflicts of interest

A. Singh was supported by the NIH T32 Training Grant (#5T32HL7381). M. Vembar and M. Grass are full-time employees of Philips Healthcare and Philips Research. V. Mor-Avi and A. Patel have received research grants from Astellas. A. Patel has received research grants from Philips and serves on the speaker's bureau for Astellas. All other authors have no relationships to disclose that would be relevant to the contents of this paper.

References

[1] U. Hoffmann, Q.A. Truong, D.A. Schoenfeld, et al., Coronary CT angiography versus standard evaluation in acute chest pain, N. Engl. J. Med. 367 (2012) 299–308.
[2] E.A. Hulten, S. Carbonaro, S.P. Petrillo, J.D. Mitchell, T.C. Villines, Prognostic value of cardiac computed tomography angiography: a systematic review and meta-analysis, J. Am. Coll. Cardiol. 57 (2011) 1237–1247.
[3] R. Blankstein, L.D. Shturman, I.S. Rogers, et al., Adenosine-induced stress myocardial perfusion imaging using dual-source cardiac computed tomography, J. Am. Coll. Cardiol. 54 (2009) 1072–1084.
[4] N. Bettencourt, A. Chiribiri, A. Schuster, et al., Direct comparison of cardiac magnetic resonance and multidetector computed tomography stress-rest perfusion imaging for detection of coronary artery disease, J. Am. Coll. Cardiol. 61 (2013) 1099–1107.
[5] T.A. Magalhaes, S. Kishi, R.T. George, et al., Combined coronary angiography and myocardial perfusion by computed tomography in the identification of flow-limiting stenosis - the CORE320 study: an integrated analysis of CT coronary angiography and myocardial perfusion, J. Cardiovasc. Comput. Tomogr. 9 (2015) 438–445.
[6] G. Pontone, G. Muscogiuri, A. Baggiano, et al., Image quality, overall evaluability, and effective radiation dose of coronary computed tomography angiography with prospective electrocardiographic triggering plus intracycle motion correction algorithm in patients with a heart rate over 65 beats per minute, J. Thorac. Imaging 33 (2018) 225–231.
[7] H. Machida, R. Fukui, J. Gao, et al., Reduction of coronary motion artifacts in prospectively electrocardiography-gated coronary computed tomography angiography using monochromatic imaging at various energy levels in combination with a motion correction algorithm on single-source fast tube voltage switching dual-energy computed tomography: a phantom experiment, Invest. Radiol. 51 (2016) 513–519.
[8] F. Tatsugami, T. Higaki, W. Fukumoto, et al., Effect of the motion correction technique on image quality at 320-detector computed tomography coronary angiography in patients with atrial fibrillation, J. Comput. Assist. Tomogr. 40 (2016) 603–608.
[9] G. Pontone, D. Andreini, E. Bertella, et al., Impact of an intra-cycle motion correction algorithm on overall evaluability and diagnostic accuracy of computed tomography coronary angiography, Eur. Radiol. 26 (2016) 147–156.
[10] J. Lessick, O. Klass, S. Wuchenauer, et al., Automatic determination of differential coronary artery motion minima for cardiac computed tomography optimal phase selection, Acad. Radiol. 22 (2015) 697–703.
[11] P. Carrascosa, A. Deviggiano, C. Capunay, M.C. De Zan, A. Goldsmit, G.A. Rodriguez-Granillo, Effect of intracycle motion correction algorithm on image quality and diagnostic performance of computed tomography coronary angiography in patients with suspected coronary artery disease, Acad. Radiol. 22 (2015) 81–86.
[12] R. Bhagalia, J.D. Pack, J.V. Miller, M. Iatrou, Nonrigid registration-based coronary artery motion correction for cardiac computed tomography, Med. Phys. 39 (2012) 4245–4254.
[13] M. Grass, A. Thran, R. Bippus, et al., Fully automatic cardiac CT motion compensation using vessel enhancement, J. Cardiovasc. Comput. Tomogr. 10 (2016) S57.
[14] P. Koken, M. Grass, Aperture weighted cardiac reconstruction for cone-beam CT, Phys. Med. Biol. 51 (2006) 3433–3448.
[15] R. Wiemker, T. Klinder, M. Bergtholdt, K. Meetz, I.C. Carlsen, T. Bulow, A radial structure tensor and its use for shape-encoding medical visualization of tubular and nodular structures, IEEE Trans. Vis. Comput. Graph. 19 (2013) 353–366.
[16] U. van Stevendaal, J. von Berg, C. Lorenz, M. Grass, A motion-compensated scheme for helical cone-beam reconstruction in cardiac CT angiography, Med. Phys. 35 (2008) 3239–3251.
[17] C.O. Schirra, C. Bontus, U. van Stevendaal, O. Dossel, M. Grass, Improvement of cardiac CT reconstruction using local motion vector fields, Comput. Med. Imaging Graph. 33 (2009) 122–130.
[18] A.A. Isola, M. Grass, W.J. Niessen, Fully automatic nonrigid registration-based local motion estimation for motion-corrected iterative cardiac CT reconstruction, Med. Phys. 37 (2010) 1093–1109.
[19] S. Leng, L. Yu, J.G. Fletcher, C.H. McCollough, Maximizing iodine contrast-to-noise ratios in abdominal CT imaging through use of energy domain noise reduction and virtual monoenergetic dual-energy CT, Radiology 276 (2015) 562–570.
[20] C.S. Chung, M. Karamanoglu, S.J. Kovacs, Duration of diastole and its phases as a function of heart rate during supine bicycle exercise, Am. J. Physiol. Heart Circ. Physiol. 287 (2004) H2003–8.
[21] R.C. Bahler, T.R. Vrobel, P. Martin, The relation of heart rate and shortening fraction to echocardiographic indexes of left ventricular relaxation in normal subjects, J. Am. Coll. Cardiol. 2 (1983) 926–933.
[22] R.W. Stafford, W.S. Harris, A.M. Weissler, Left ventricular systolic time intervals as indices of postural circulatory stress in man, Circulation 41 (1970) 485–492.
[23] A.M. Weissler, W.S. Harris, C.D. Schoenfeld, Systolic time intervals in heart failure in man, Circulation 37 (1968) 149–159.